Microstructure basis for strong piezoelectricity in Pb-free $Ba(Zr_{0.2}Ti_{0.8})O_3$-$(Ba_{0.7}Ca_{0.3})TiO_3$ ceramics

Jinghui Gao,[1,3,a)] Dezhen Xue,[1,2,3] Yu Wang,[1] Dong Wang,[1,2] Lixue Zhang,[1,2] Haijun Wu,[1,2] Shengwu Guo,[2] Huixin Bao,[1,2] Chao Zhou,[1] Wenfeng Liu,[1] Sen Hou,[1,2] Ge Xiao,[1,2] and Xiaobing Ren[1,3,a)]

[1]*Multi-disciplinary Materials Research Center, Frontier Institute of Science and Technology, State Key Lab of Electrical Insulation and Power Equipment, Xi'an Jiaotong University, Xi'an 710049, China*
[2]*State Key Lab for Mechanical Behaviors of Materials, Xi'an Jiaotong University, Xi'an 710049, China*
[3]*Ferroic Physics Group, National Institute for Materials Science, Tsukuba, Ibaraki 305-0047, Japan*

(Received 22 July 2011; accepted 6 August 2011; published online 29 August 2011)

In this letter, we use transmission electron microscopy to study the microstructure feature of recently reported Pb-free piezoceramic $Ba(Zr_{0.2}Ti_{0.8})O_3$-$x(Ba_{0.7}Ca_{0.3})TiO_3$ across its piezoelectricity-optimal morphotropic phase boundary (MPB) by varying composition and temperature, respectively. The domain structure evolutions during such processes show that in MPB regime, the domains become miniaturized down to nanometer size with a domain hierarchy, which coincides with the d_{33}-maximum region. Further convergent beam electron diffraction measurement shows that rhombohedral and tetragonal crystal symmetries coexist among the miniaturized domains. Strong piezoelectricity reported in such a system is due to easy polarization rotation between the coexisting nano-scale tetragonal and rhombohedral domains. © *2011 American Institute of Physics*. [doi:10.1063/1.3629784]

Piezoceramics, which can convert mechanical stress into electrical charge and vice versa, have been found various applications in industry and daily life.[1] However, such materials are now facing a big challenge: they over-rely on a Pb-based material $Pb(ZrTi)O_3$ (PZT), which has excellent piezoelectric performance but strong toxicity. Therefore, many efforts have been made worldwide to search for a good Pb-free substitute for PZT.[2–5] Recent reported Pb-free $Ba(Zr_{0.2}Ti_{0.8})O_3$-$(Ba_{0.7}Ca_{0.3})TiO_3$ (BZT-BCT) solid solution[6] is one promising piezoelectric system: for the composition locating in proximity to a ferroelectric-ferroelectric morphotropic phase boundary (MPB) of such a system, the piezoelectric coefficient d_{33} has been reported up to 560-620pC/N, which is comparable with that of high-end or soft PZT ($d_{33} = 500$-600 pC/N).

It has long been recognized that ferroelectric domains play an important role in the piezoelectric performance of material. Therefore, intensive studies have been focused on domain structures and the corresponding crystallographic features[7–16] of PZT and other Pb-based piezoelectric systems, such as $Pb(Mg_{1/3}Nb_{2/3})O_3$-$PbTiO_3$ (PMN-PT) and $Pb(Zn_{1/3}Nb_{2/3})$ O_3-$PbTiO_3$ (PZN-PT). It is found that domain structures of these systems show a common feature: high-piezoelectric-response MPB composition always coincides with a "miniaturized domain structure,"[10–16] which manifests itself as an "adaptive phase"[14,15] consisting of nanodomains. Such a microstructure feature indicates a low polarization anisotropy[17,18] caused by phase instability and thus suggests a good piezoelectric performance. Despite of the studies in Pb-based piezoelectrics, in the Pb-free BZT-BCT system with PZT-comparable piezoelectric performance, microstructure basis is still missing. In this letter, we investigate the reason for strong piezoelectricity in BZT-BCT system from the microstructure evolution around its MPB composition through transmission electron microscope (TEM). The observed domain structure in such a high-d_{33} Pb-free piezoelectric system shows great similarity with Pb-based materials.[10–16] This may provide a microstructure guide for developing ultra-high performance Pb-free piezoelectrics.

The $Ba(Zr_{0.2}Ti_{0.8})O_3$-$x(Ba_{0.7}Ca_{0.3})TiO_3$ ($x = 0.4$-0.6) ceramics for TEM observation were prepared by using the raw chemicals of $BaZrO_3$ (98%), $CaCO_3$ (99.9%), $BaCO_3$ (99.95%), and TiO_2 (99.9%). Calcining was done at 1350 °C for 3 h followed by sintering at 1450 °C for 3 h. The samples were then prepared following a conventional method of mechanical thinning, dimpling, and ion milling to electron transparency before TEM observation. Room-temperature TEM observation was done by using a JEM-2010 microscope with acceleration voltage of 200 kV and convergent beam electron diffraction (CBED) measurement with 5 nm probe size was used to determine the crystal symmetry. Further cold-stage TEM observation was performed on a JEM-2000FX microscope at 200 kV.

The phase diagram of BZT-BCT (established by Liu and Ren[6]) suggests that two pseudo-binaries BZT and BCT exhibit symmetry-lowering transitions from high-temperature paraelectric cubic phase (C) to low-temperature ferroelectric rhombohedral (R) and tetragonal (T) phases with spontaneous polarizations $\boldsymbol{P_S}$ align along [111] and [100], respectively. MPB locates at the transition region between R and T. We study such a ferroelectric-ferroelectric transition going through MPB by two approaches: varying composition x (along the horizontal line in Fig. 1(a)) as well as varying temperature t (along the vertical line in Fig. 1(a)) to achieve the "composition-induced" and "temperature-induced" R-MPB-T transition, respectively.

a)Authors to whom correspondence should be addressed. Electronic addresses: GAO.Jinghui@nims.go.jp and REN.Xiaobing@nims.go.jp.

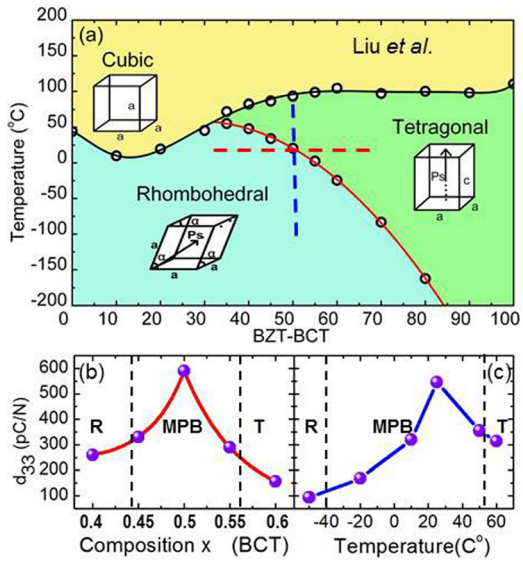

FIG. 1. (Color online) (a) Phase diagram of $Ba(Zr_{0.2}Ti_{0.8})O_3$-x$(Ba_{0.7}Ca_{0.3})$-TiO_3 (BZT-xBCT) around MPB composition (after Liu *et al.*[6]). (b) Composition-dependence of d_{33} during composition-induced R-MPB-T transition along horizontal line (red) in (a)). (c) Temperature-dependence of d_{33} during temperature-induced R-MPB-T transition along vertical line (blue) in 1(a)).

Piezoelectric coefficient d_{33} of our samples have been measured during such composition-induced and temperature-induced transitions. The changing of d_{33} during composition-induced transition ($t = 25\,^{\circ}C$ and $x = 0.4$-0.6) measured by a Berlincourt-type meter shows a peak at the MPB composition with x = 0.5 (Fig. 1(b)). On the other hand, the evolution of d_{33} on temperature-induced transition ($x = 0.5$ and $t = -50$-$60\,^{\circ}C$) was measured by using a resonance technique[19] with a HIOKI impedance analyzer. It shows a maximum d_{33} in MPB regime with $t = 25\,^{\circ}C$ (Fig. 1(c)). Such results of our samples are similar to those of the previous studies.[6,20] It is clear from Figs. 1(b) and 1(c) that MPB in BZT-BCT system enhances the piezoelectric coefficient d_{33} to 2-6 times than the one in its pure R or T phase.

Bright field (BF) TEM images in Figs. 2(a)–2(c) show the microstructure evolution during the R-MPB-T transition when varying composition ($x = 0.4$, 0.5, and 0.6) at room temperature 25 °C. All the images were taken with the electron-beam incident direction of pseudo cubic [001]. It can be seen that BZT-rich ($x = 0.4$) sample has a typical rhombohedral domain structure (Fig. 2(a)), while BCT-rich ($x = 0.6$) sample exhibits a symbolic tetragonal structure (Fig. 2(c)), both in micron size. More important result comes from the intermediate MPB composition (x = 0.5) which exhibits a unique microstructure (Fig. 2(b)): the micron-sized domain lamellas can still be roughly observed. However, the distinct feature of MPB composition is that miniaturized nanodomains with the average size of 20-100 nm are developed on these lamellas forming a "domain hierarchy."[13,14] The enlargement of dash-squared area inside one domain lamella is shown in the inset of Fig. 2(b) with clear nanodomain structure. Therefore, microstructure study on composition-induced R-MPB-T transition shows a micron-nano-micron evolution in domain structure, and high-d_{33} MPB composition coincides with a miniaturized nanodomains structure with a domain hierarchy.

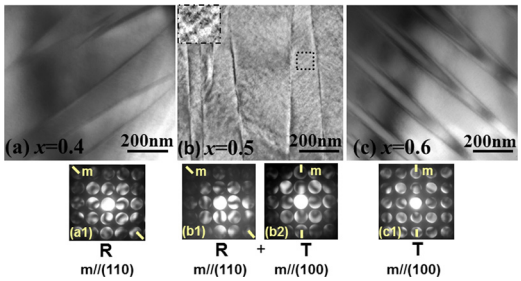

FIG. 2. (Color online) TEM observation of composition-induced R-MPB-T transition in BZT-xBCT ($t = 25\,^{\circ}C$ and $x = 0.4$, 0.5, and 0.6). The BF image of BZT-xBCT from $[001]_{PC}$ incidence (a)$x = 0.4$, (b) $x = 0.5$, and (c) $x = 0.6$. (a1) The CBED pattern obtained from one domain in (a), indicating R symmetry. (b1) and (b2) The CBED pattern obtained from one domain lamella in (b), indicating coexistence of R and T symmetry in MPB region. (c1) The CBED pattern obtained within one domain in (c), indicating T symmetry.

To further investigate the local crystal symmetry of samples, we applied CBED diffraction technique, which can detect the point group symmetry in minuscule region. Two ferroelectric binaries in the phase diagram show rhombohedral and tetragonal symmetries, with the point group of 3 m and 4 mm, respectively. It is quite easy to differentiate them in the projection-diffraction CBED pattern from [001] incidence:[14] rhombohedral 3 m point symmetry has (110) or $(\bar{1}10)$ mirror plane, while tetragonal 4 mm point symmetry has (010) or (100) mirror plane. Fig. 2(a1) shows the CBED pattern of x = 0.4 sample, which exhibits clear (110) mirror plane suggesting a rhombohedral symmetry. On the other hand, x = 0.6 sample exhibits a (001) mirror showing a tetragonal symmetry (Fig. 2(c1)). Nevertheless, the BZT-0.5BCT shows a different crystallographic characteristic: two sets of mirrors (110) and (100) appear among the miniaturized nanodomains within one domain lamella (Figs. 2(b1) and 2(b2)), which suggests that R and T crystal symmetries coexist among these nanodomains. Therefore, during the composition-induced transition the microstructure evolves from R to T via the mixture of nano R and T at d_{33}-maximum MPB regime.

Moreover, the microstructure evolution for temperature-induced transition has also been observed for the BZT-0.5BCT composition sample (x = 0.5). The BF image during *in-situ* cooling TEM observation has been shown in Fig. 3. At 60 °C, the sample exhibits micron-sized tetragonal domain structure (Fig. 3(a)). When cooling the sample to 25 °C of MPB temperature (Fig. 3(b)), interestingly, domain lamellas of T phase are inherited. However, the distinct feature is that the miniaturized nanodomains develop on these lamellas, which can be clearly seen in the inset of Fig. 3(b) as an enlargement of dash-squared area. It is highly likely that during cooling R nanodomains grow inside the T domain lamellas, which lead to a coexisting of T and R phase in nanometer scale indicated by CBED measurement in Figs. 2(b1) and 2(b2). On further cooling (−180 °C), a micron-sized rhombohedral domain structure (Fig. 3(c)) completely replaces MPB domain structure. Therefore, the *in-situ* cooling TEM observation for temperature-induced R-MPB-T transition also shows a micron-nano-micron evolution in microstructure and domains miniaturized down to nanometer scale in the d_{33}-maximum MPB regime.

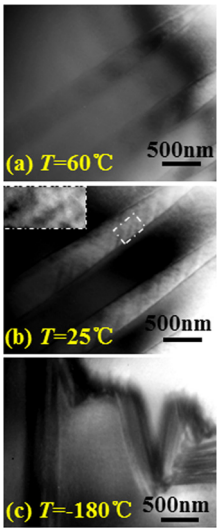

FIG. 3. (Color online) *In-situ* cooling TEM observation of temperature-induced reverse R-MPB-T transition (x = 0.5 and $t = -180$, 25, and 60 °C) in BZT-0.5BZT from $[001]_{PC}$ incidence. (a) BF image at $t = 60$ °C shows a tetragonal domain structure. (b) BF image at $t = 25$ °C shows a miniaturized nanodomain structure with a domain hierarchy. (c) BF image at $t = -180$ °C shows a rhombohedral domain structure.

It should be noted that our observed minaturized nanodomain structure shows great similarity to the domain morphology of PZT,[10–12] PMN-PT (Refs. 13–15), and PZN-PT,[15,16] which has been considered as the microstructure feature of MPB in Pb-based piezoelectrics with strong piezoelectricity. In addition, such a domain structure has also been found in several MPB-type Pb-free piezoelectric systems.[21,22] In the present paper, by studying the microstructure evolution in combination with d_{33} evolution during composition-induced and temperature-induced R-MPB-T transition, we proves that the miniaturized nanodomain structure corresponds well with high piezoelectric performance in the Pb-free BZT-BCT system and they frequently go hand in hand. We also realize from temperature-induced R-MPB-T transition results (Figs. 1(c) and 3) that the temperature stability of BZT-BCT system is quite poor. Better substitutions may lie in the systems with higher curie temperature[29] and PZT-like temperature-independent MPB, which also exhibit minaturized nanodomains in microstructure. Such a domain structure and its relationship with strong piezoelectricity in BZT-BCT system can be well understood by thermodynamic analysis of MPB.

The thermodynamic theory of MPB was established by Haun *et al.*,[23,24] Ishibashi *et al.*,[25] Rossetti *et al.*[17] and Kachaturyan.[18] In our BZT-BCT piezoelectric system, MPB line starts from a tricritical-triple point (as shown in Fig. 1(a)), which is a critical point[6,26] bordering the discontinuous and continuous transition. It thus corresponds with an isotropic free energy state. And in the MPB line deviating from such a point with two ferroelectric phase equilibrium, a low degree of polarization anisotropy energy can be expected. This can thus lead to two deductions. First, the low anisotropy energy will result in a drastic reduction of the domain wall energy. Classical domain theory points out that such domain wall energy (F_{DW}) can determine size of domains (D) by $D \propto \sqrt{F_{DW}}$. Accordingly, the corresponding domains have been miniaturized in MPB regime, as has been observed in Figs. 2(b) and 3(b). Second, the piezoelectricity is enhanced due to low polarization anisotropy on MPB. The low polarization anisotropy leads to a low energy barrier between two ferroelectric phases, and thus facilitates the rotation[27,28] between the coexisting R ($\boldsymbol{P_S}$||[111]) and T ($\boldsymbol{P_S}$||[100]) phase which leads to strong piezoelectricity in our BZT-BCT system. It should be noted that another possible critical contributor may lie in the polarization extention/contraction[30] between ferroelectric phase (T or R) and paraelectric phase (C) due to low curie temperature.

The authors thank K. Otsuka, T. Suzuki, X. D. Ding, S. Yang, R. H. Zhu, Y. H. Li, Y. M. Zhou, J. K. Deng, Z. Zhang, Y. C. Ji, D. C. Lv, and X. Q. Ke for helpful discussions. This work was supported by Kakenhi of JSPS, National Natural Science Foundation of China (Grant No. 51072158, 51007070, and 51071117), National Basic Research Program of China under Grant No. 2010CB613003, Fundamental Research Funds for Central Universities of China as well as NCET and 111 project of China.

[1]K. Uchino, *Ferroelectric Devices* (Marcel Dekker, New York, 2000).
[2]T. R. Shrout and S. J. Zhang, J. Electroceram. **19**, 113 (2007).
[3]J. Rodel, W. Jo, K. Seifert, E. Anton, T. Granzow, and D. Damjanovic, J. Am. Ceram. Soc. **92**, 1153 (2009)
[4]Y. Saito, H. Takao, T. Tani, T. Nonoyama, K. Takatori, T. Homma, T. Nagaya, and M. Nakamura, Nature **432**, 84 (2004).
[5]T. Takenaka and H. Nagata, J. Eur. Ceram. Soc. **25**, 2693 (2005).
[6]W. Liu and X. Ren, Phys. Rev. Lett. **103**, 257602 (2009).
[7]B. Noheda, D. E. Cox, G. Shirane, J. A. Gonzalo, L. E. Cross, and S-E. Park, Appl. Phys. Lett. **74**, 2059 (1999).
[8]A. A. Bokov and Z. G. Ye, J. Appl. Phys. **95**, 6347 (2004).
[9]A. M. Glazer, P. A. Thomas, K. Z. Baba-Kishi, G. K. H. Pang, and C. W. Tai, Phys. Rev. B. **70**, 184123 (2004).
[10]D. I. Woodward, J. Knudsen, and I. M. Reaney, Phys. Rev. B **72**, 104110 (2005).
[11]R. Theissmann, L. A. Schmitt, J. Kling, R. Schierholz, K. A. Schönau, H. Fuess, M. Knapp, H. Kungl, and M. J. Hoffmann, J. Appl. Phys. **102**, 024111 (2007).
[12]K. A. Schonau, L. A. Schmitt, M. Knapp, H. Fuess, R. A. Eichel, H. Kungl, and M. J. Hoffmann, Phys. Rev. B **75**, 184117 (2007).
[13]F. Bai, J. F. Li, and D. Viehland, Appl. Phys. Lett **85**(12), 2313 (2004).
[14]H. Wang, J. Zhu, N. Lu, A. A. Bokov2, Z.-G. Ye, and X. W. Zhang, Appl. Phys. Lett. **89**, 042908 (2006).
[15]Y. M. Jin, Y. U. Wang, A. G. Khachaturyan, J. F. Li, and D. Viehland, Phys. Rev. Lett. **91**, 197601 (2003).
[16]U. Belegundu and K. Uchino, Ferroelectr. Lett. **26**, 107 (1999).
[17]G. A. Rossetti, A. G. Khachaturyan, G. Akcay, and Y. Ni, J. Appl. Phys. **103**, 114113 (2008).
[18]A.G. Khachaturyan, Philos. Mag. **90**, 37 (2010).
[19]IEEE standard on piezoelectricity, 54 (1988).
[20]D. Xue, Y. Zhou, H. Bao, C. Zhou, J. Gao, and X. Ren, J. Appl. Phys. **109**, 054110 (2011).
[21]J. Yao, L. Yan, W. Ge, L. Luo, J. Li, and D. Viehland, Phys. Rev. B **83**, 054107 (2011).
[22]L. A. Schmitt, M. Hinterstein, H. Kleebe, and H. Fuess, J. Appl. Cryst. **43**, 805 (2010).
[23]M. J. Haun, E. Furman, S. J. Jang, and L. E. Cross, Ferroelectrics **99**, 13 (1989).
[24]D. Damjanovic, J. Am. Ceram. Soc. **88**, 2663 (2005).
[25]Y. Ishibashi and M. Iwata, Jpn. J. Appl. Phys. **37**, L985 (1998).
[26]M. Porta and T. Lookman, Phys. Rev. B **83**, 174108 (2011).
[27]H. X. Fu and R. E. Cohen, Nature (London) **403**, 281 (2000).
[28]M. Ahart, M. Somayazulu, R. E. Cohen, P. Ganesh, P. Dera, H.-k. Mao, R. J. Hemley, Y. Ren, P. Liermann, and Z. Wu, Nature (London) **451**, 545 (2008).
[29]H. Bao, C. Zhou, D. Xue, J. Gao, and X. Ren, J. Phys. D: Appl. Phys. **43**, 465401 (2010).
[30]D. Damjanovic, Appl. Phys. Lett. **97**, 062906 (2010).